ISSN (Print) 1226-1750
ISSN (Online) 2233-6656
Journal of Magnetics 27(2), 132-140 (2022) https://doi.org/10.4283/JMAG.2022.27.2.132

Research on Magnetic Field of Multistage Counter Roll Magnetorheological Fluid Transmission Device

Xiangfan Wu[1], Yangyang Guo[2], Zuzhi Tian[2]*, Fangwei Xie[2], and Yujie Tang[2]

[1]*School of Mechanical and Electrical Engineering, Xuzhou University of Technology, Xuzhou, 221018, China*
[2]*School of Mechanical and Electrical Engineering, China University of Mining and Technology, Xuzhou, 221116, China*

(Received 29 March 2022, Received in final form 16 June 2022, Accepted 18 June 2022)

Aiming to solve the problem of magnetorheological transmission heat dissipation, a novel magnetorheological fluid transmission device is designed, and the torque of the device is analyzed. Based on electromagnetic theory, the magnetic circuit of the device is designed. The finite element method is used to simulate the magnetic field of the measurement device. Results show that the working magnetic induction can reach 0.5 T when the current is 1.6 A, which can meet design requirements. The magnetic induction intensity in the working space increases with the increase of the excitation current and permeability of the magnetic conductive material; decreases with the increase of the size of the working space; and increases with the increase of the size of the magnetic ring. The magnetic induction intensity in the working area is DT4C, 20 steel, and 45 steel from strong to weak. The experimental results are consistent with the simulation.

Keywords : magnetorheological transmission, torque analysis, multistage counter roll, simulation of magnetic field

1. Introduction

Magnetorheological (MR) fluid is composed of soft magnetic particles, carrier fluids, and stabilizers; It is a kind of intelligent material. MR transmission technology is a novel type of power transmission technology developed by using MR fluid as a transmission medium [1-5]. The shear yield stress of MR fluid is adjusted by controlling the intensity of the applied magnetic field, and then the transfer torque speed is adjusted [6, 7]. When the intensity of the applied magnetic field changes continuously in a certain range, the continuous shear stress corresponding to the intensity of the magnetic field can be obtained, and the step-less control of torque and speed can be realized [8, 9].

However, MR fluid working temperature is usually between −20 °C to 150 °C. The traditional dual MR fluid transmission device is subjected to high strength shear stress in the process of power transmission. The soft magnetic particles in each layer move relative to each other and generate a lot of friction heat after curing which leads to the serious heat of the MR fluid in the working gap. The rheological characteristics of the MR fluid decline sharply [10-13]. It is an urgent problem to design an effective method to limit the temperature rise of MR fluid.

Numerous scholars proposed various solutions to address the problems. Pisuwala investigated the effect of magnetic nanoparticles on the thermal conductivity of MR fluid [14]. Dogruoz adopted a method of mounting a heat sink on an MR damper housing to improve heat dissipation efficiency [15]. Wang used water cooling through the device within the channel to carry out cooling, but the design of the flow channel was complex [16]. Ji improved the cooling effect of the MR fluid clutch transmission disc by designing the guide column group of cooling units [17]. Du added an aluminum foil bubble insulation material with low thermal conductivity in the cavity between the electromagnetic coil and the MR fluid to avoid rapid temperature rise [18].

The traditional magnetorheological fluid transmission device adopts a disc transmission structure. During the transmission process, the magnetorheological fluid is in slip mode for a long time, and the work efficiency is low due to serious heating. In the roller drive mode, the magnetorheological fluid in the drive area decreases and it is basically no-slip, and the heat generation decreases accordingly. Therefore, this paper innovatively designed a

*Corresponding author: Tel: +86-13914876762
Fax: +86-0516-83590777, e-mail: tianzuzhi@163.com

multistage counter roll MR fluid transmission device. The torque of the transmission device is analyzed based on the viscoplastic constitutive equation of Bingham fluid, and the magnetic circuit of the device is designed based on electromagnetic theory. The simplified magnetic circuit model is simulated by finite element analysis, and the influence of the magnetic circuit on the MR fluid transmission device is determined.

2. Analysis of Transmission Torque

Fig. 1a shows the 3D model of the multistage counter roll MR fluid transmission device and Fig. 1b shows the schematic diagram of a set of roll pair drives and the working gap has been enlarged for convenient analysis. Table 1 shows the main spatial dimensions of the MR device.

Based on the viscoplastic constitutive equation of Bingham fluid, the shear yield stress of MR fluid is given as:

$$\tau = \tau_0(B)\,\mathrm{sgn}(\dot{\gamma}) + \eta\dot{\gamma} \tag{1}$$

Suppose that the radius of the main and driven drum are

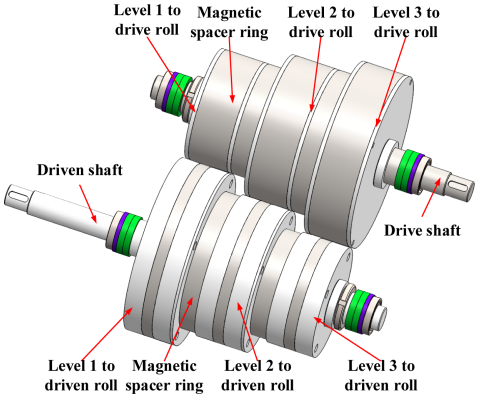

(a) Model of MR fluid transmission device

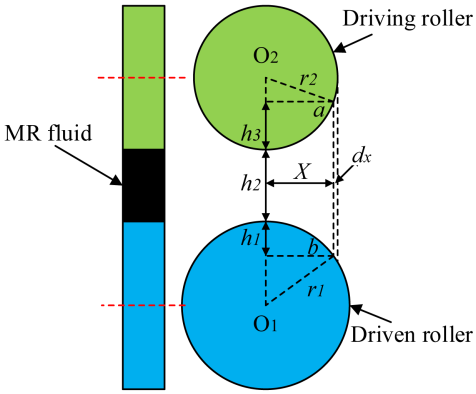

(b) Schematic diagram of a set of roll pair drive

Fig. 1. (Color online) Establishment of transmission model and analysis model.

Table 1. Main spatial dimensions of the device.

Part	Material	Parameter
drive roll 1 (driven roll 3)	20 steel	R=70 mm Width: 60 mm
drive roll 2 (driven roll 2)	20 steel	R=90 mm Width: 60 mm
drive roll 2 (driven roll 2)	20 steel	R=110 mm Width: 60 mm
Magnetic spacer ring (drive)	Aluminum alloy	Width: 50 mm
Magnetic spacer ring (driven)	Aluminum alloy	Width: 25 mm
Coil	cooper	800 turn
Work space	/	1.5 mm

r_1 and r_2, the angular velocity of the active drum is ω_1, the angular velocity of the driven drum is ω_2, and the width of the drum is L. MR fluid fills the working gap, then:

$$\frac{\omega_1}{\omega_2} = \frac{r_2}{r_1} \tag{2}$$

Suppose the horizontal velocities of the master and slave rollers at points a and b are respectively V_a and V_b, and the distance between a and b from the center lines of the two rollers is X, x_1 is half of the horizontal curing distance of MR fluid between two rollers, then V_a and V_b and the torque T of single-stage roller-pair drive can be approximated as:

$$V_a = \sqrt{r_1^2 - x^2}\,\omega_1 \tag{3}$$

$$V_b = \sqrt{r_2^2 - x^2}\,\omega_2 \tag{4}$$

$$T = 2\int_0^{x_1} (r_1 + h_2/2)(\tau_0(B) + \eta\dot{\gamma})L dx \tag{5}$$

$$T = 2\int_0^{x_1} (r_1 + h_2/2)\tau_0(B)L dx + 2\int_0^{x_1} (r_1 + h_2/2)\eta\dot{\gamma} L dx \tag{6}$$

The latter part of the formula is the viscous torque of MR fluid, which can be ignored. The total torque can be expressed as:

$$T_m = 2(r_1 + h_2/2)\tau_0(B)Lx_1 \tag{7}$$

Where $\tau_0(B)$ is the inherent characteristics of MR fluid, r_1, h_2 and L are the sizes of MR fluid transmission device, and x_1 is related to the properties of MR fluid and magnetic field strength selected. The maximum theoretical transfer torque is 8 N·m.

3. Design of Magnetic Circuit

MR fluid transmission device components of the device

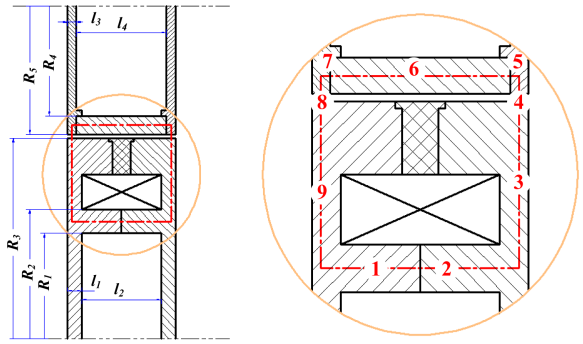

Fig. 2. (Color online) Structure diagram of the magnetic circuit.

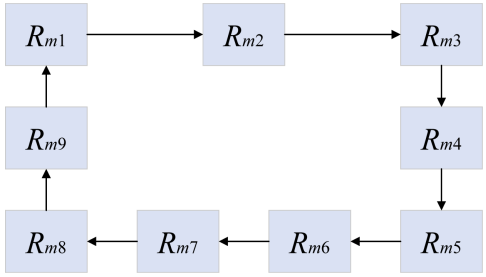

Fig. 3. (Color online) Schematic diagram of magnetic resistance.

structure for material selection and magnetic field strength are crucial. The content of the magnetic circuit design demonstrates that the MR fluid transmission device mainly includes magnetically permeable material and magnetic insulation material. The magnetic circuit materials are generally made of magnetic material to ensure the passage of magnetic field lines. The non-magnetic part of the material is generally composed of magnetic material to avoid magnetic leakage.

Fig. 2 schematically illustrates the designed magnetic circuit of the MR fluid transmission device based on the structural characteristics of the MR fluid transmission device and the design requirements of the magnetic field. As shown in Fig. 2, to simplify the calculation, the transmission region is selected for analysis. And the magnetic circuit can be divided into the following 9 parts: 1 for the driving left shell, 2 for the driving right shell, 3 and 9 for the MR fluid in the driving area, 4 and 8 for the flow gap, 5 for the right baffle plate of the driven roller, 7 for the left baffle plate of the driven roller, and 6 for the driven roller.

Based on Ohm's law for magnetic circuit, the magnetic resistance of each part of the magnetic circuit is given as:

$$R_{mk} = \frac{l_k}{\mu_k A_{0k}} \tag{8}$$

Where l corresponds to the magnetic circuit length, μ is the permeability of the magnetic circuit material, A represents the cross-sectional area of the magnetic circuit, and k is the number of magnetic circuits.

Fig. 3 shows the schematic diagram of magnetic resistance of a single-stage pair roll magnetic circuit. According to Eq. (8) and considering the size indicated in Fig. 2, the reluctance of each section of the magnetic circuit can be obtained as Eq. (9). Where R_j (j=1~5) represents the radial size of the driving and driven roller, l_1~l_4 represent the axial size of each part in the magnetic circuit and μ_1~μ_9 represent the permeability of each part of the material in the magnetic circuit.

$$R_{m2} = \frac{(l_1+l_2)/2}{\mu_2(R_2-R_1)\Delta x} \quad R_{m1} = \frac{(l_1+l_2)/2}{\mu_1(R_2-R_1)\Delta x}$$

$$R_{m3} = \frac{R_3-(R_1+R_2)/2}{\mu_3 l_1 \Delta x} \quad R_{m4} = \frac{0.0015}{\mu_4 l_1 \Delta x}$$

$$R_{m5} = \frac{l_3/2}{\mu_5(R_5-R_4)\Delta x} \quad R_{m6} = \frac{l_4}{\mu_6(R_5-R_4)\Delta x}$$

$$R_{m7} = \frac{l_3/2}{\mu_7(R_5-R_4)\Delta x} \quad R_{m8} = \frac{0.0015}{\mu_8 l_1 \Delta x}$$

$$R_{m9} = \frac{R_3-(R_1+R_2)/2}{\mu_9 l_1 \Delta x} \tag{9}$$

According to the above formula, the total reluctance in the magnetic circuit of one-stage roller pair can be expressed as:

$$R_m = \sum_{k=1}^{9} R_{mk} \tag{10}$$

According to ohm's law of the magnetic circuit, the magnetic flux can be given as:

$$\Phi = \frac{NI}{R_m} = \frac{NI}{\sum_{k=1}^{9} R_{mk}} \tag{11}$$

In an ideal state, the magnetic flux in all parts of the magnetic circuit is theoretically equal:

$$\Phi = \Phi_4 = B_4 S_4 = B_4 l_1 \Delta x \tag{12}$$

Where B_4 represents the magnetic induction intensity in the working area of the single-stage roll pair and S_4 represents the effective flux area of the working area of the roll. The total magnetomotive force of the excitation coil of the one-stage pair of rollers is:

$$NI = R_m \Phi = R_m B_4 l_1 \Delta x \tag{13}$$

The magnetic circuit reluctance is related to the structure and material of the magnetic circuit. The magnetomotive force needed to reach the designed magnetic flux density can be calculated according to Eq. (13) after the total reluctance is determined. The main parameters of the coil are then determined. The calculated total magnetic force of the one-stage pair of rollers is about 708, and the ampere-turns of the excitation coil is 800.

4. Analysis of Magnetic Field

ANSYS software using the scalar method for magnetic circuit simulation is used to analyze the rationality of the magnetic circuit design. MR fluid transmission device components of the material properties can be divided into four categories, wherein the relative permeability of magnetic insulation materials, such as stainless steel, brass, air and cooling water, take an approximate value of 1. In magnetic materials of 20 steel, 45steel, DT4C, and MR fluid are nonlinear materials. Their relative permeability is defined by the B-H curve, as shown in Fig. 4.

On the premise of not affecting the simulation results, the electromagnetic model is simplified as follows: the influence of bolts, nuts and keyways on the magnetic circuit is ignored, and the complex parts are simplified appropriately. The simplified 1/2 3D MR fluid transmission device model is shown in the Fig. 5.

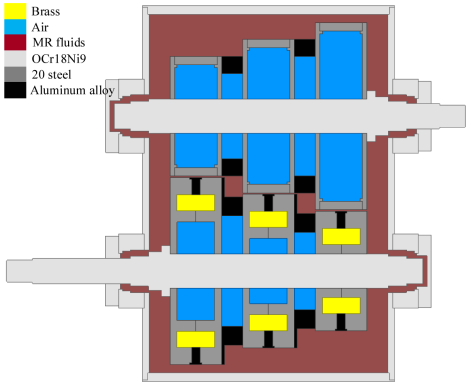

Fig. 5. (Color online) Simplified 3D model of 1/2 MRF transmission device.

The finite element software is used to simulate the model and the total magnetic field distribution of the MR

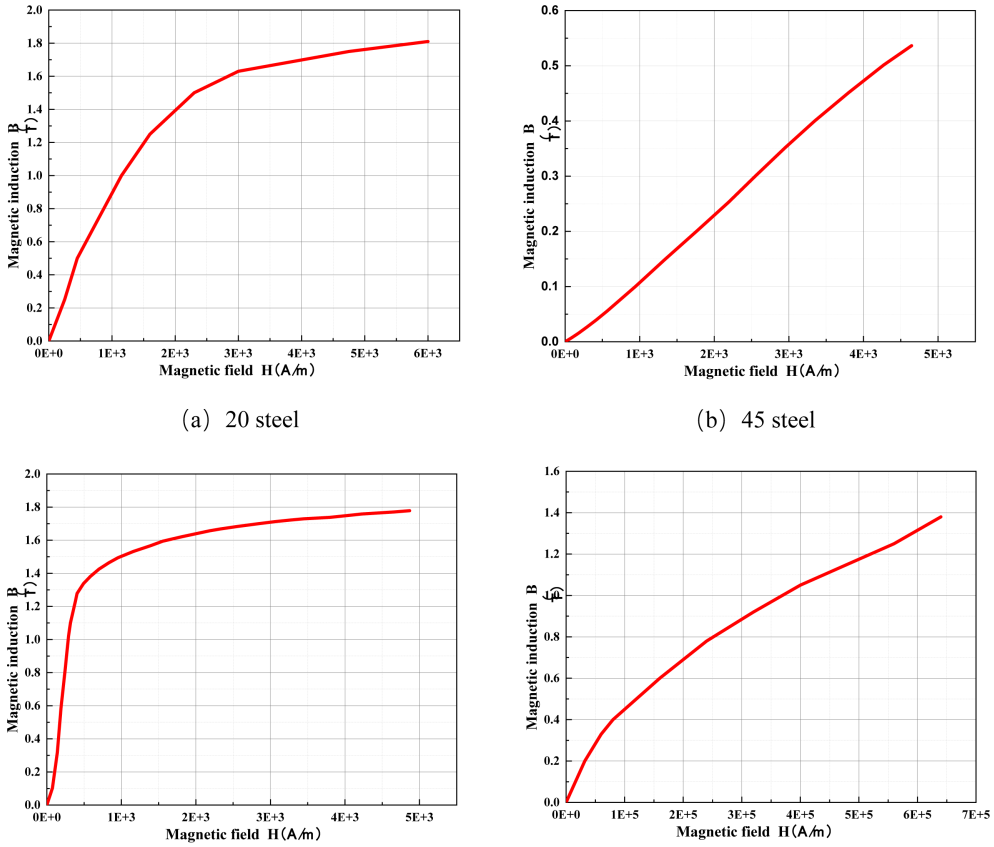

(a) 20 steel (b) 45 steel

(c) DT4C (d) MR fluid

Fig. 4. (Color online) B-H curves of nonlinear materials.

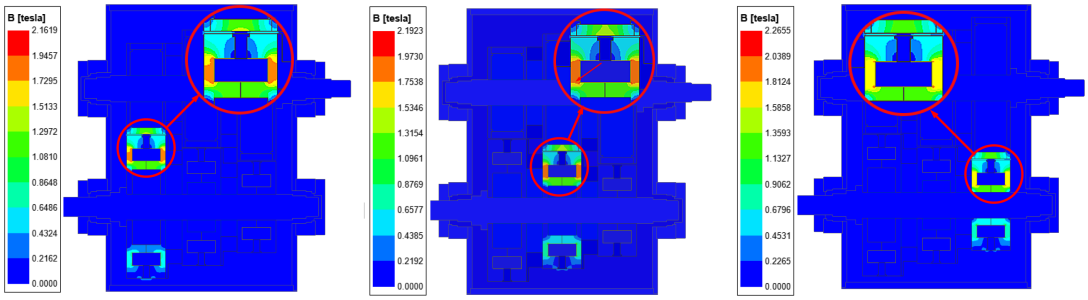

(a) Level 1 to roll (b) Level 2 to roll (c) Level 3 to roll

Fig. 6. (Color online) Magnetic induction intensity distribution diagram.

fluid transmission device is obtained. The magnetic induction intensity distribution is shown in Fig. 6.

The magnetic induction intensity distribution diagram of the three pairs of rollers shows that the magnetic induction intensity on the left and right sides of the excitation coil is significantly higher than that on other parts of the transmission process. The magnetic induction intensity in the working area is basically greater than 0.5T, which meets the working requirements of MR fluid. In the three groups, the magnetic induction intensity at other non-conductive parts such as the spacer magnetic ring is low, which plays a good barrier and constraint role on the magnetic field lines. The magnetic circuit design is reasonable.

5. Analysis of Influencing Factors of Magnetic Induction Intensity

5.1. Excitation coil current

The second stage roll pair is taken as the analysis object to explore the influence of excitation coil current on magnetic induction intensity in the working area of the governor. The number of coil turns is set to 500 under the condition that other parameters remain unchanged, the current variation range is 1.2 A~1.8 A, and the interval is 0.2 A. Fig. 7 and 8 show the magnetic induction intensity curve and magnetic induction intensity distribution cloud diagram in the working area of the second roller group under different currents.

The magnetic induction intensity of the working area increases with the increase of excitation current. Its variation trend is nonlinear, but due to the nonlinear material of the magnetic circuit, with the increase of excitation current, its variation trend gradually decreases and tends to saturation. When the current is greater than 1.6 A, the magnetic induction intensity reaches the working point of MR fluid (0.5 T).

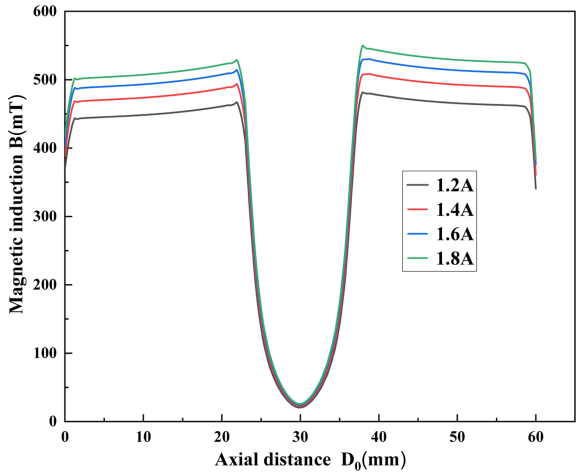

Fig. 7. (Color online) Magnetic induction intensity curve of the working area under different current.

5.2. Working area size of MR fluid

In order to explore the influence of working area size on magnetic induction intensity, the second stage roll pair is taken as the analysis object. The number of coil is set to 500 turns under the condition that other parameters remain unchanged, and set the three working area size to 1mm, 1.5 mm and 2 mm for magnetic field analysis. Fig. 9 and Fig. 10 show the magnetic induction intensity curve and magnetic induction intensity distribution cloud diagram.

When the size of the working area increases from 1 mm to 2 mm, the maximum magnetic induction intensity of the governor decreases first and then increases. When the size of the working area is less than or equal to 1.5 mm, the magnetic induction intensity of the working area meets the working condition of MR fluid (0.5 T).

The magnetic induction intensity of the working area decreases with the increase of the size of the working area, because the increase of the size of the working area leads to the increase of magnetic circuit reluctance, which leads to the decrease of magnetic induction intensity.

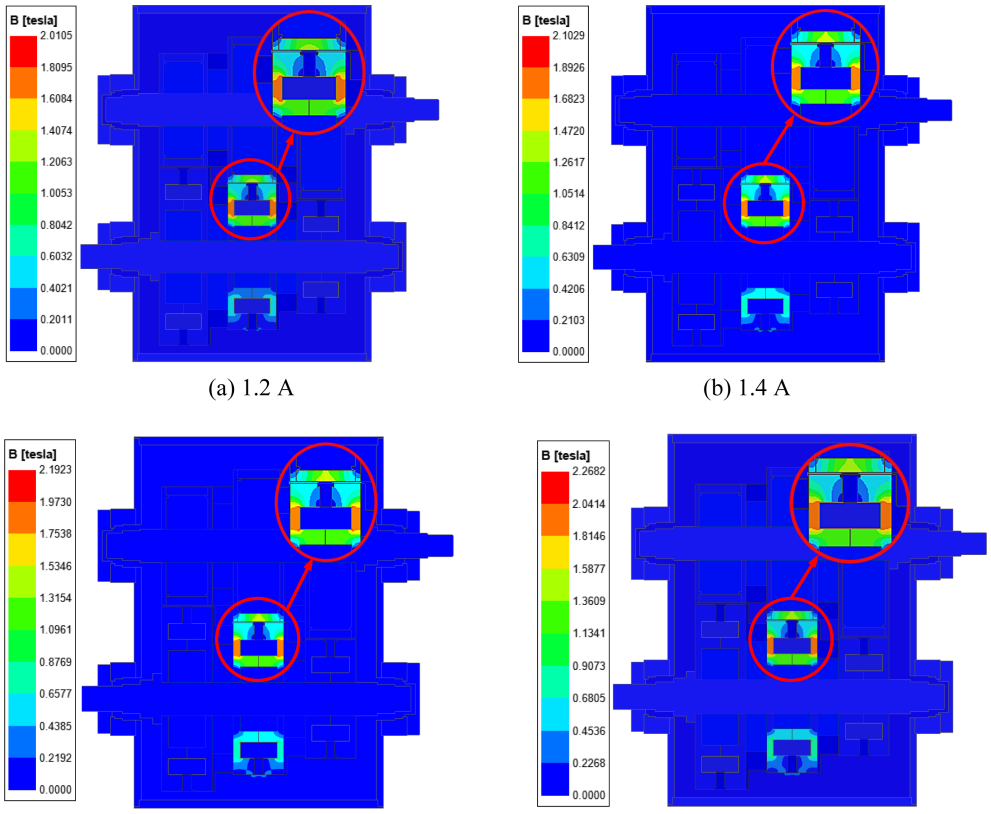

Fig. 8. (Color online) Cloud diagram of magnetic induction intensity distribution under different currents.

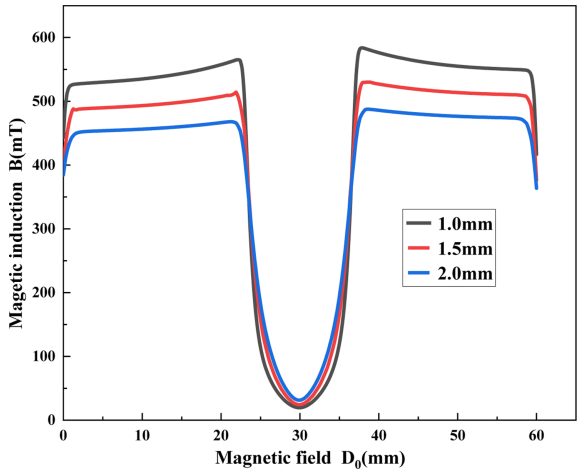

Fig. 9. (Color online) Magnetic induction intensity curves.

5.3. Different size of magnetic separator ring

Fig. 11 shows the magnetic induction intensity curve and Fig. 12 shows the distribution cloud diagram of magnetic induction intensity in the working area under the second roller. The size of magnetic separation ring is 5 mm, 10 mm, and 15 mm. The number of turns of the excitation coil is 500, and the current is 1.6 A. With the size of the magnetic ring increases from 5 mm to 15 mm, the maximum magnetic induction intensity of the governor first decreases and then increases, which is caused by the accumulation of local magnetic field lines in the magnetic circuit when the size of the magnetic ring increases. When the size of the magnetic separation ring is greater than 10 mm, the magnetic induction intensity in the working area meets the working condition of MR fluid (0.5 T).

5.4. Roller material

The magnetic induction intensity in the working area of the MR transmission device has a great influence on the selection of roller materials. Three common materials (20 steel, 45 steel, and pure electric iron) in the market are selected for comparative analysis.

Fig. 13 shows the magnetic induction intensity curve and Fig. 14 shows the distribution cloud diagram of magnetic induction intensity in the working area under the second roller. Highest gathered in excitation coil and the magnetic induction intensity of the initiative to contact roller shell to the corner, subordinate to the roll material for DT4C and 20 steel in the interval of the

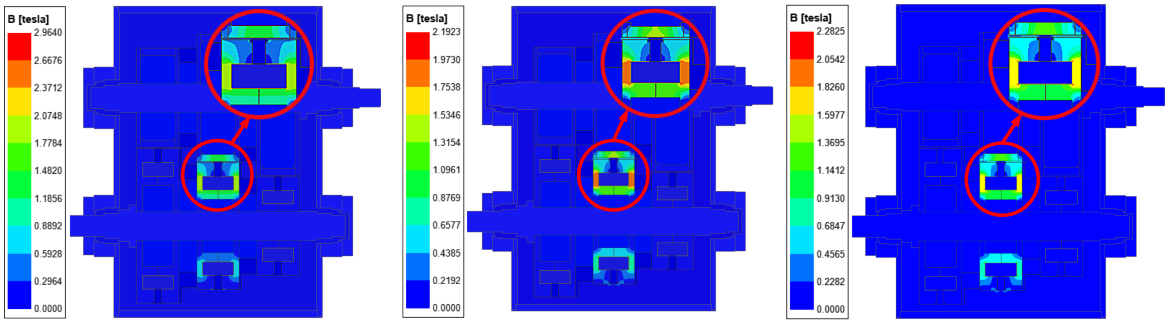

(a) 1.0mm (b) 1.5mm (c) 2.0mm

Fig. 10. (Color online) Cloud diagram of magnetic induction intensity distribution under different working area sizes.

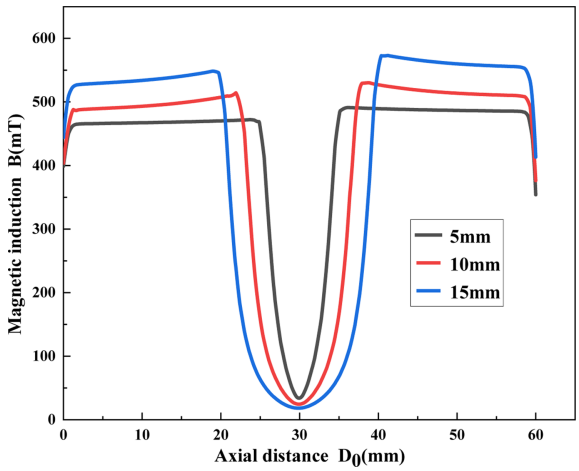

Fig. 11. (Color online) Magnetic induction intensity curve under different sizes of the magnetic spacer ring.

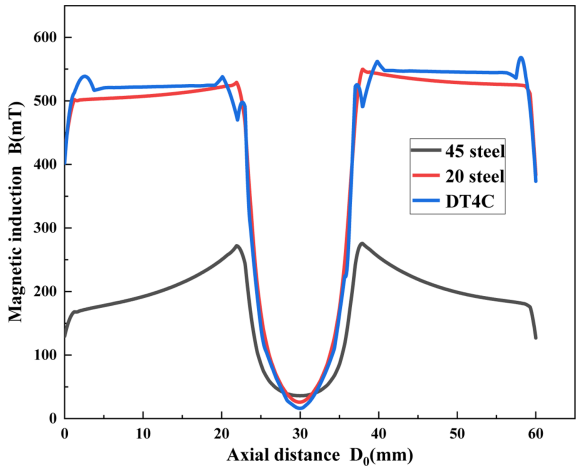

Fig. 13. (Color online) Magnetic induction intensity curve of master-slave counter roll under different materials.

circular location to stretch, the magnetic induction intensity declined slightly, subordinate to the roll material of 45 steel in the interval of the circular location to stretch, the magnetic induction intensity in a downward trend.

The magnetic induction intensity of the working area of the three materials used for roller is DT4C, 20 steel and 45 steel in descending order, among which DT4C and 20 steel meet the working requirements of MR fluid. Considering the complexity and high price of DT4C processing, 20 steel is the best material choice.

6. Experiment and Result Analysis

In order to verify the correctness of the simulation results and check whether the MR fluid transmission device design is reasonable. As shown in Fig. 15, an

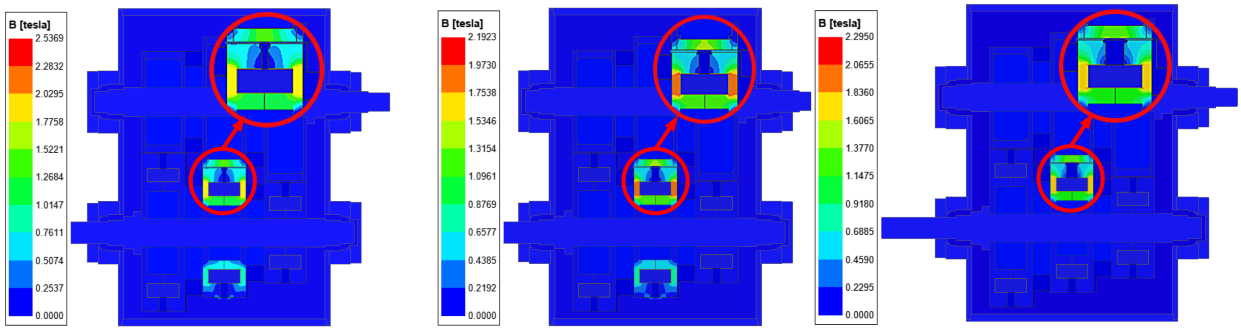

(a) 5 mm (b) 10 mm (c) 15 mm

Fig. 12. (Color online) Cloud diagram of magnetic induction intensity distribution under different sizes of magnetic spacer ring.

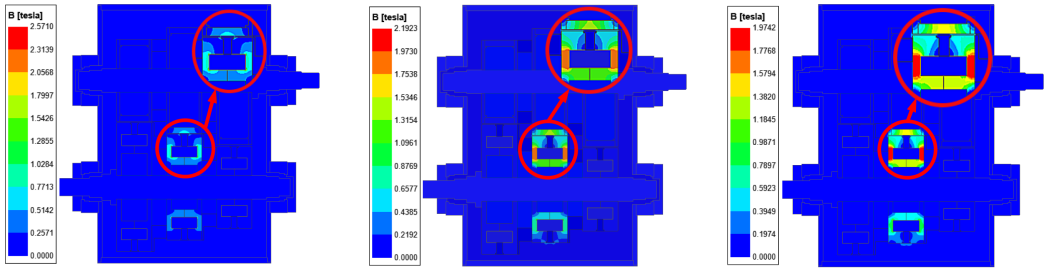

(a) 45steel (b) 20steel (c) DT4C

Fig. 14. (Color online) Cloud diagram of magnetic induction distribution under different materials of master-slave counter roll.

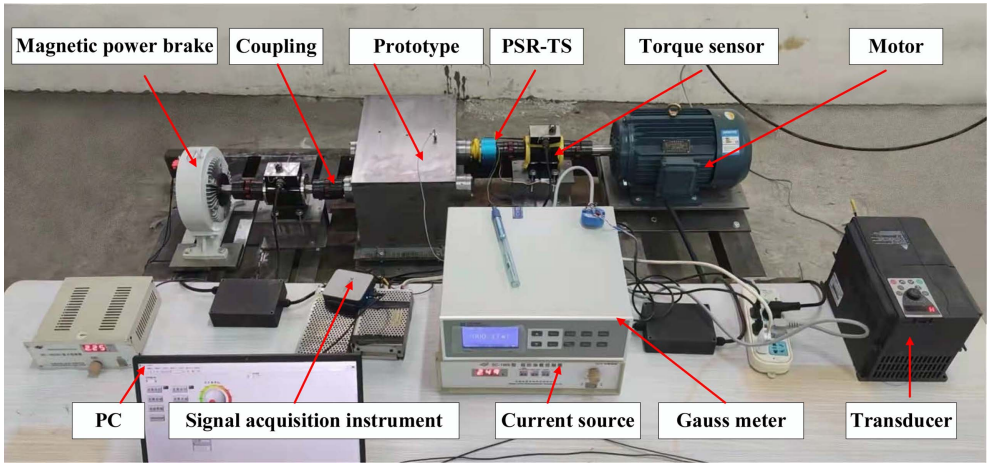

Fig. 15. (Color online) Experimental test-bed.

experimental test-bed for MR fluid transmission device is set up. It consists of motor, torque sensor, PSR-TS, prototype, coupling, magnetic power brake, PC, signal acquisition instrument, current source, gauss meter, transducer, etc. Mechanical transmission part includes: three-phase asynchronous motor used to provide system power, torque sensor used to measure speed torque signal, coupling connecting two different mechanisms, PSR-TS used to ensure the power supply of the governor coil, magnetic powder brake used to apply load and prototype. The data acquisition and control part includes: a programmable current source for adjusting the current of the governor's excitation coil to change the size of the governor's internal magnetic field, magnetic powder brake used to adjust the size of magnetic powder brake torque, the PC side of the computer for controlling and collecting signals.

During the magnetic induction intensity characteristic experiment, the magnetic field intensity can be changed by adjusting the programmed current source, and the magnetic induction intensity in the working area can be measured by gauss meter. The current in the excitation coil rises from 0.5 A to 3 A at intervals of 0.5 A.

Fig. 16 shows that the magnetic induction intensity in the working area increases with the increase of the current in the excitation coil. When the current in the coil is greater than 2.5 A, the magnetic induction intensity in the working area is greater than 0.5 T. The magnetic induction intensity of MR fluid in the working area is slightly lower than the simulation result. Actually, there is

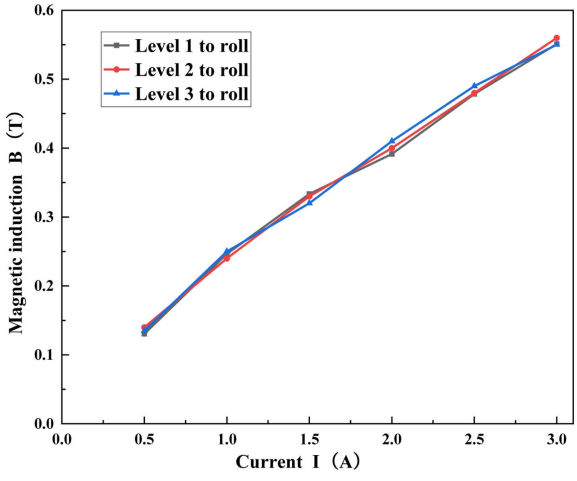

Fig. 16. (Color online) Magnetic induction characteristics.

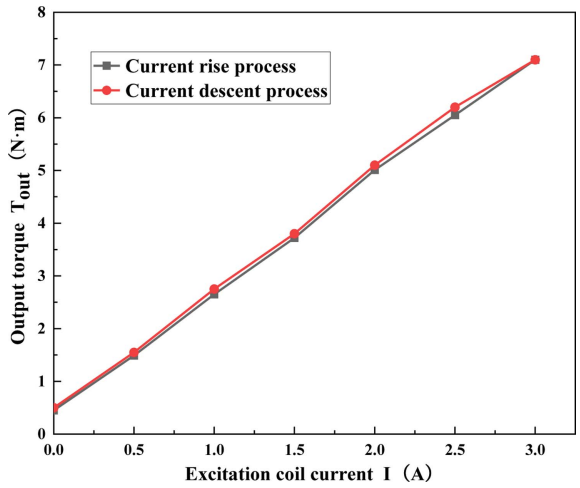

Fig. 17. (Color online) Output torque and current relationship curve.

a magnetic leakage phenomenon in the device. There is a certain error between the magnetic permeability of MR fluid used and the theoretical value.

To obtain the relationship between output torque and current, the speed was set as 50 r/min, and the output current of programmed current source was adjusted to increase from 0 A to 3 A and then decrease from 3 A to 0 A at an interval of 0.5 A.

Fig. 17 shows that the maximum output torque is about 7 N·m. With the increase or decrease of the excitation coil current, the output torque of the transmission device increases or decreases correspondingly. However, the output torque in the process of coil current decline is slightly higher than that in the process of coil current rise, because a small amount of remanence occurs in the magnetic circuit.

The comparison between the experimental results and the simulation results shows that they are basically consistent, indicating that the design of the multistage counter roll MR fluid transmission device is reasonable.

7. Conclusions

The magnetic circuit is simulated by finite element software ANSYS. Results show that: the shear stress generated by MR fluid is effectively applied as most of the magnetic force lines pass vertically through the working area of MR fluid. In the middle of the axial direction of the magnetic field intensity, the magnetic induction intensity decreases obviously. The highest magnetic induction intensity is concentrated at the contact corner between the excitation coil and the active roller housing. When the current is greater than 1.6 A, the magnetic induction intensity of MR fluid in the working area reaches the working point (0.5 T).

The influences of current, size of working area, size of magnetic separator ring and roll material on transmission performance are analyzed. Experimental results are in good agreement with the simulation results.

Acknowledgment

This research was supported by the National Natural Science Foundation of China (52005426, 51875560), Jiangsu Natural Science Foundation (BK20190155) and the Priority Academic Program Development of Jiangsu Higher Education Institutions.

References

[1] M. Jiang, X. T. Rui, F. F. Yang, W. Zhu, and Y. N. Zhang, J. Intell. Mater. Syst. Struct. **33**, 33 (2022).
[2] W. Sun, J. J. Yu, and Y. R. Cai, J. Intell. Mater. Syst. Struct. **31**, 2312 (2020).
[3] C. Y. Gao, Q. Liu, H. J. Choi, N. H. Kim, and C. Y. You, J. Magn. **24**, 162 (2019).
[4] P. J. Widodo, E. P. Budiana, and U. Ubaidilah, Appl. Sci. **11**, 9807 (2021).
[5] Y. Rabban, M. Ashtiani, and S. H. Hashemabadi, Soft. Matter. **11**, 4453 (2015).
[6] M. Ashtiani, S. H. Hashemabadi, and A. Ghaffari, J. Magn. Magn. Mater. **374**, 716 (2015).
[7] Y. H. Huang, Y. H. Jiang, X. B. Yang, and R. Z. Xu, J. Magn. **20**, 317 (2015).
[8] X. F. Wu, X. M. Xiao, Z. Z. Tian, and F. Chen, J. Magn. **24**, 634 (2019).
[9] M. D. Christie, S. Sun, J. H. Quenzer, L. Deng, H. Deng, and W. H. Li, J. Smart. Mater. Strut. **30**, 045013 (2021).
[10] S. Y. Wang, F. Chen, Z. Z. Tian, J. Dou, and X. F. Wu, J. Smart. Mater. Strut. **23**, 285 (2018).
[11] G. Q. Liang, T. Zhao, N. F. Li, Y. T. Wei, and S. M. Savaresi, J. Smart. Mater. Strut. **30**, 125005 (2021).
[12] Z. M. Fu, X. Gan, X. H. Liu, Z. Jian, and H. N. Hu, J. Chin. Insti. Engin. **45**, 97 (2022).
[13] Z. Z. Tian, C. W. Guo, F. Chen, and X. F. Wu, J. Magn. **22**, 281 (2017).
[14] M. S. Pisuwala, R. V. Upadhyay, and K. Parekh, J. Appl. Phy. **126**, 722 (2019).
[15] S. R. Patil, K. P. Powar, and S. M. Sawant, J. Appl. Therm. Eng. **98**, 238 (2016) .
[16] D. M. Wang, B. Zi, Y. Zeng, Y. F. Hou, and Q. R. Meng, J. Mater. Sci. **49**, 8459 (2014).
[17] J. J. Ji, Z. Z. Tian, X. F. Wu, and J. Dou, J. Magn. **23**, 93 (2018).
[18] C. B. Du, F. N. Zeng, and B. Liu, J. Smart. Mater. Strut. **30**, 075001 (2021).